Relativistic analysis of meson exchange currents in elastic electron-deuteron scattering

E. Hummel and J. A. Tjon
Institute for Theoretical Physics, University of Utrecht, 3508 TA Utrecht, The Netherlands
(Received 6 March 1990)

The $\rho\pi\gamma$ and $\omega\varepsilon\gamma$ meson exchange current contributions to the deuteron form factors are calculated in a relativistic quasipotential one-boson-exchange model. Recoil corrections to the two-body EM current operator are kept. It is shown that a substantial reduction of the $\rho\pi\gamma$ graph occurs especially at high momentum transfer as compared to the usual nonrelativistic treatment, where only leading-order terms in p/M are retained. As a consequence, the $\omega\varepsilon\gamma$ contribution becomes also important at high momentum transfer. Using the value for the $\omega\varepsilon\gamma$ coupling constant from a relativistic quark model, the elastic EM form factors are predicted in reasonable accordance with the experimental data.

I. INTRODUCTION

In the past considerable effort has been made to reconstruct two nucleon interactions from the nucleon-nucleon scattering data. Besides more phenomenological approaches such as in the case of the Reid interaction, within a meson theoretical framework a highly successful description has been achieved from the two nucleon interaction which is able to describe the nucleon-nucleon data up to a few hundred MeV Lab energy. Additional information can in principle be extracted from the study of elastic electron scattering on nuclear systems, the deuteron being the most simple one. However, with increasing energy and momentum transfer effects of subnucleonic degrees of freedom and special relativity are expected to play an important role.

Several estimates have been made in the literature of the mesonic exchange current (MEC) contributions. For the deuteron the so-called pair term and the $\rho\pi\gamma$ graph contribution have been shown the most important ones. Within a nonrelativistic approach these calculations appear to agree very well with the Saclay[1] and the SLAC (Ref. 2) data, but the MEC corrections tend to shift the dip to too high momentum transfer as compared to the recent SLAC data[3] for the magnetic form factor. On the other hand, from studies of relativistic models[4–6] in the relativistic impulse approximation based on the one-boson-exchange (OBE) approach, it has been clear that a consistent treatment of both the nucleon-nucleon dynamics and the electromagnetic (EM) interaction is needed in order to get a reliable estimate of the effects of special relativity. In particular, the pair term is grossly canceled by a correction, depending on the NN dynamics. Therefore an analysis of the MEC contributions within a relativistic approach is obviously of interest.

In the usual treatment of the MEC contributions it is implicitly assumed that the kinetic motion of the nucleons can be neglected as compared to their mass. As a consequence the resulting effective EM operator becomes a local one and therefore facilitates the computation of these contributions. However, at higher momentum transfers such an approximation is expected not to be valid any more and recoil corrections have to be included. In this paper we study the relativistic two-loop $\rho\pi\gamma$ contribution within a quasipotential OBE model, in order to see how well such a local approximation is. In addition, since we are using the same strong vertex form factors in both the EM calculation and the nucleon-nucleon dynamics the analysis is at least consistently done within a same model. Recently an estimate[7] was made of the effective $\omega\varepsilon\gamma$ coupling due to vacuum polarization corrections in a relativistic quantum hadron dynamical (QHD) model, indicating that such a contribution to MEC may also be important. For this reason we have also examined in our relativistic model the $\omega\varepsilon\gamma$ graph.

In Sec. II we give the relativistic expressions of the vertex operator of the $\rho\pi\gamma$ graphs including the boost effects. The helicity formalism is used to describe the deuteron wave function. Employing a quasipotential approximation the current is simplified in Sec. III. In particular the nonrelativistic limit is discussed. The results of the fully relativistic calculations are described in Sec. IV. Negative energy state contributions and boost effects are found to be small, rendering the so-called static approximation to be good. Compared to the usual nonrelativistic calculations based on the effective local EM two-body operators, the magnetic form factor of the $\rho\pi\gamma$ graph falls much faster. The result is that the deuteron magnetic form factor is less sensitive to the $\rho\pi\gamma$ contribution as usually found. For the electric form factors of the MEC the effects are not as large but still substantial. The $\omega\varepsilon\gamma$ graph is discussed in Sec. IV. With the chosen coupling constant, the contribution is found to be important and comparable to the $\rho\pi\gamma$ contribution. The $\omega\varepsilon\gamma$ MEC brings the deuteron EM form factors in better agreement with the experimental data.[8] For the deuteron form factors the complete results including the impulse approximation (IA) are described in Sec. V. We also investigate in this section the sensitivity of the IA to the different nucleon form factors. In the final section some concluding remarks are made.

II. THE $\rho\pi\gamma$ GRAPH

In the one-photon exchange approximation, the elastic EM form factors of the deuteron can be expressed in terms of the deuteron current. Denoting the deuteron bound-state wave function with total four momentum P and polarization M by $|P,M\rangle$, the current matrix element is given by

$$\langle P',M'|J_\mu(q)|P,M\rangle=\frac{1}{2M_D(2\pi)^7}\int d^4p\int d^4p'\bar{\Phi}_D^{(M')}(p';P')S_2(p',P')\Gamma_\mu(q,P',p',P,p)S_2(p,P)\Phi_D^{(M)}(p;P)\ , \tag{2.1}$$

where $S_2(p,P)=i(\frac{1}{2}\not{P}+\not{p}-m)^{-1}i(\frac{1}{2}\not{P}-\not{p}-m)^{-1}$ is the two nucleon Green's function and Γ_μ is the EM vertex operator at momentum transfer q, while p,p' are the relative four momenta in the initial and final state. In the impulse approximation Γ_μ is simply related to the one nucleon current operator. It is given in that case by $(2\pi)^4\Gamma_\mu(q)S^{(2)^{-1}}(\frac{1}{2}P'+p')\delta(p'-p-\frac{1}{2}q)$, where the EM coupling is given by

$$\Gamma_\mu(q)=e(F_1^S\gamma_\mu+\frac{i}{2M_N}F_2^S\sigma_{\mu\nu}q^\nu)\ . \tag{2.2}$$

The deuteron vertex function $\Phi_D^{(M)}$ satisfies the homogeneous Bethe-Salpeter equation, which has formally the form

$$\Phi_D^{(M)}=VS_2\Phi_D^{(M)}\ , \tag{2.3}$$

where V represents the interaction between the two nucleons. For the relativistic OBE model the normalization of $\Phi_D^{(M)}$ is given by

$$2P_\mu\delta_{M,M'}=\frac{i}{4\pi^3}\int d^4p\,\bar{\Phi}_D^{(M)}(p;P)\times\left[\frac{\partial}{\partial P_\mu}S_2(p,P)\right]_{P^2=M_D^2}\Phi_D^{(M')}(p;P) \tag{2.4}$$

in accordance with the correct value of the current at $q^2=0$. In a relativistic field theory[4,5] based on meson exchanges, the elastic EM form factors have been studied in detail in the impulse approximation using both the Bethe-Salpeter equation and quasipotential approximations to it. Contributions due to meson exchange currents have been examined in the literature,[9,10] showing that the $\rho\pi\gamma$ graphs given in Fig. 1, contribute significantly at high momentum transfer. The structure of Γ_μ for the $\rho\pi\gamma$ graph can be found from the following Lagrangians:

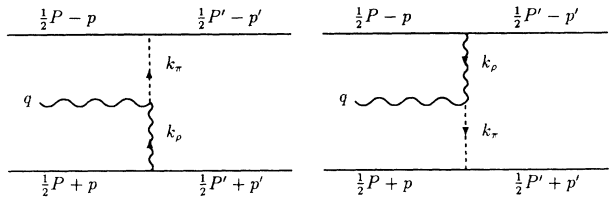

FIG. 1. The $\rho\pi\gamma$ meson exchange current diagrams.

$$L_{\pi NN}=-g_{\pi NN}^{PV}\bar{u}(p)\gamma_5\gamma_\mu\tau\cdot\partial^\mu\pi u(p')\ ,$$

$$L_{\rho NN}=g_{\rho NN}^{V}\bar{u}(p)\left[\gamma_\mu-\frac{g_{\rho NN}^{T}}{2M_N}\sigma_{\mu\nu}\partial^\nu\right]\tau\cdot\rho^\mu u(p')\ , \tag{2.5}$$

$$L_{\rho\pi\gamma}=-e\frac{g_{\rho\pi\gamma}}{2m_\rho}\epsilon_{\alpha\beta\gamma\delta}F^{\alpha\beta}(\rho^\gamma\cdot\partial^\delta\pi)$$

with $\epsilon_{0123}=-1$ and where the strong meson-nucleon form factors F are assumed to be of the monopole form

$$F_\pi(k)=F_\rho(k)=(1-k^2/\Lambda^2)^{-1} \tag{2.6}$$

with Λ the cut-off mass. For the form factor of the $\rho\pi\gamma$ vertex we use vector dominance,[11] i.e.,

$$F_{\rho\pi\gamma}(k)=(1-k^2/m_\omega^2)^{-1}\ , \tag{2.7}$$

where m_ω is the mass of the ω meson. For the vertex of Fig. 1(a) we have

$$\Gamma_\mu^{(1)}=-iC_{\rho\pi\gamma}\left[\gamma_\lambda(1)-\frac{ig_{\rho NN}^{T}}{2M_N}\sigma_{\lambda\nu}(1)k_\rho^\nu\right]\times\left[-g^{\lambda\sigma}+\frac{k_\rho^\lambda k_\rho^\sigma}{m_\rho^2}\right]\epsilon_{\mu\alpha\beta\sigma}q^\alpha k_\pi^\beta\gamma_5(2)\not{k}_\pi\tau_1\cdot\tau_2\ , \tag{2.8}$$

where

$$C_{\rho\pi\gamma}=eg_{\rho NN}^{V}g_{\pi NN}^{PV}\frac{g_{\rho\pi\gamma}}{m_\rho}F_\pi(k_\pi)F_\rho(k_\rho)\times F_{\rho\pi\gamma}(q)\Delta_\pi(k_\pi)\Delta_\rho(k_\rho) \tag{2.9}$$

and Δ_π and Δ_ρ are the scalar part of the propagators of the π and ρ meson, i.e., $\Delta_n=(k^2-m_n^2)^{-1}$. The expressions for Fig. 1(b) are very similar: just replace k_π and k_ρ by the ones defined in Fig. 1(b). Due to the antisymmetric Levi-Civita symbol $\epsilon_{\mu\alpha\beta\sigma}$ the $\rho\pi\gamma$ MEC contribution satisfies gauge invariance.

The analysis of Eq. (2.1) proceeds in a similar way as in Ref. 4 for the single nucleon current operator. To relate the current operator to the EM form factors it is convenient to calculate Eq. (2.1) in the Breit frame, i.e., $\mathbf{P}+\mathbf{P}'=0$. From $P+q=P'$ follows that $\mathbf{P}'=-\mathbf{P}=\frac{1}{2}\mathbf{q}$ and $q_0=0$. Since the deuteron vertex function is most easily obtained from the dynamical equations in the c.m. frame, a boost transformation to the Breit system is needed. We have

$$\Phi_D^{(M)}(p;P)=\Lambda^{(1)}(\mathcal{L})\Lambda^{(2)}(\mathcal{L})\Phi_D^{(M)}(\mathcal{L}^{-1}p;\mathcal{L}^{-1}P) \tag{2.10}$$

and

$$S(p,P)=\Lambda(\mathcal{L})S(\mathcal{L}^{-1}p,\mathcal{L}^{-1}P)\Lambda^{-1}(\mathcal{L}) , \tag{2.11}$$

where $\mathcal{L}^{-1}$ is the Lorentz transformation to the c.m. frame and $\Lambda(\mathcal{L})=\Lambda^{(1)}(\mathcal{L})\Lambda^{(2)}(\mathcal{L})$ the corresponding boost operator for spin-$\frac{1}{2}$ particles. Let us now define the intrinsic c.m. variables k and k' by $k=\mathcal{L}^{-1}p$ and $k'=\mathcal{L}'^{-1}p'$. We may now shift all the effects of the boosts to the EM operator Γ_μ. As a result we can rewrite the current [only the contribution of Fig. 1(a)] to

$$\langle P',M'|J_\mu^{\rho\pi\gamma}(q)|P,M\rangle=\frac{1}{2M_D(2\pi)^7}\int d^4k\int d^4k'\bar{\Phi}_D^{(M')}(k';P_{\text{c.m.}})S_2(k',P'_{\text{c.m.}})\tilde{\Gamma}_\mu^{(1)}(q,k',k)S_2(k,P_{\text{c.m.}})\Phi_D^{(M)}(k;P_{\text{c.m.}}) , \tag{2.12}$$

where

$$\tilde{\Gamma}_\mu^{(1)}(q,k',k)=\Lambda^{-1}(\mathcal{L}')\Gamma_\mu^{(1)}(q,p',p)\Lambda(\mathcal{L}) . \tag{2.13}$$

Taking $\mathbf{q}=(0,0,q)$ the Lorentz transformation is defined by

$$\mathcal{L}'^{-1}P'=\mathcal{L}^{-1}P=(M_D,\mathbf{0})=P_{\text{c.m.}} , \tag{2.14}$$

where

$$\mathcal{L}_\mu^\nu=\begin{bmatrix}\sqrt{1+\eta} & 0 & 0 & -\sqrt{\eta}\\ 0 & 1 & 0 & 0\\ 0 & 0 & 1 & 0\\ -\sqrt{\eta} & 0 & 0 & \sqrt{1+\eta}\end{bmatrix}, \quad \eta=\frac{\mathbf{q}^2}{4M_D^2} \tag{2.15}$$

and $\mathcal{L}'=\mathcal{L}^{-1}$. In the Breit frame the boost operator for spin-$\frac{1}{2}$ particles is given by

$$\Lambda(\mathcal{L})=\left[\frac{E_D+M_D}{2M_D}\right]^{1/2}\left[1+\gamma^0\gamma^3\frac{P}{E_D+M_D}\right] , \tag{2.16}$$

where P is the component in the z direction and $E_D=(P^2+M_D^2)^{1/2}$ the energy of the deuteron. The vertex $\Gamma_\mu^{(1)}$ can be worked out to give for the charge operator

$$J_0(k_\pi,k_\rho)=-C_{\rho\pi\gamma}\left[\gamma(1)+\frac{g_{\rho NN}^T}{4M_N}[\gamma(1)\not{k}_\rho-\not{k}_\rho\gamma(1)]\right]q\gamma_5(2)\not{k}_\pi\boldsymbol{\tau}_1\cdot\boldsymbol{\tau}_2 , \tag{2.17}$$

where $\gamma(1)=i[k_\pi^1\gamma^2(1)-k_\pi^2\gamma^1(1)]$, and for the current operator $J_+=J_1+iJ_2$

$$\begin{aligned}J_+(k_\pi,k_\rho)=-C_{\rho\pi\gamma}\Bigg[&\left[\gamma^0(1)+\frac{g_{\rho NN}^T}{4M_N}[\gamma^0(1)\not{k}_\rho-\not{k}_\rho\gamma^0(1)]\right]q(k_\pi^1+ik_\pi^2)\\&-\left[\gamma_+(1)+\frac{g_{\rho NN}^T}{4M_N}[\gamma_+(1)\not{k}_\rho-\not{k}_\rho\gamma_+(1)]\right]qk_\pi^0\Bigg]\gamma_5(2)\not{k}_\pi\boldsymbol{\tau}_1\cdot\boldsymbol{\tau}_2 ,\end{aligned} \tag{2.18}$$

where $\gamma_+(1)=\gamma^1(1)+i\gamma^2(1)$.

Expression Eq. (2.12) for the deuteron current can explicitly be evaluated by substituting the expansion Eq. (A11) of the nucleon propagator in the helicity spinors. Together with the definition of the deuteron vertex function [Eq. (A12)] on this helicity basis the deuteron current can be written in the form

$$\langle P',M'|J_\mu^{\rho\pi\gamma}(q)|P,M\rangle=\frac{1}{2M_D(2\pi)^7}\int d^4k\int d^4k'\sum_{a',a}\bar{\phi}^{(M')}(k';a)S_{\rho_1',\rho_2'}(k')\tilde{\Gamma}^{(1)}_{\mu,a',a}S_{\rho_1,\rho_2}(k)\phi^{(M)}(k;a) , \tag{2.19}$$

where

$$\tilde{\Gamma}^{(1)}_{\mu,a',a}=\bar{V}^{\rho_1'}_{\lambda_1'}(\mathbf{k}')\bar{V}^{\rho_2'}_{\lambda_2'}(\mathbf{k}')\tilde{\Gamma}^1_\mu V^{\rho_2}_{\lambda_2}(\mathbf{k})V^{\rho_1}_{\lambda_1}(\mathbf{k}) \tag{2.20}$$

and $a=\{\lambda_1,\lambda_2,\rho_1,\rho_2\}$. The two nucleon propagator S_{ρ_1,ρ_2} depends only on the ρ-spin indices ρ_1 and ρ_2.

Within the helicity and ρ-spin formalism, we may introduce (see Appendix A) for the deuteron the partial wave state components $\phi_{n,m}(\mathbf{k},k_0)$ labeled by the quantum number $n=\{J,M,L,S\}$ and $m=\{\lambda_1,\lambda_2,\rho\}$. This last label combines ρ_1 and ρ_2 in $a=\{\lambda_1,\lambda_2,\rho_1,\rho_2\}$, where ρ represents the total energy spin of the NN system as defined in Eq. (A15). On this ρ-spin basis the two nucleon propagator is given by Eq. (A19) and the deuteron current can be expressed as

$$\langle P',M'|J_\mu^{\rho\pi\gamma}|P,M\rangle=\frac{1}{2M_D(2\pi)^7}\int dk_0\int dk\,k^2\int d\cos\theta\int d\varphi\int dk_0'\int dk'k'^2\int d\cos\theta'\int d\varphi'$$
$$\times\sum_{n,n'}\sum_{m,m'}\sum_{\tilde\rho'\tilde\rho}\bar\phi_{n',m'}(\mathbf{k}',k_0)S_{\rho'\bar\rho'}(k')\tilde\Gamma^{(1)}_{\tilde m',\tilde m}S_{\bar\rho\rho}(k)\phi_{n,m}(\mathbf{k},k_0)\,, \quad (2.21)$$

where $\tilde m=\{\lambda_1,\lambda_2,\tilde\rho\}$. As compared to Eq. (2.19) we have an extra summation of the indices $\tilde\rho$ and $\tilde\rho'$, due to the fact that the two nucleon propagator is not diagonal in the total ρ spin. The matrix elements $\tilde\Gamma^{(1)}_{\tilde m',\tilde m}$ can simply be constructed from Eq. (2.20) by the recoupling of ρ_1 and ρ_2 to ρ.

Using the parity transformation property of the wave function as given by Eq. (A22) and interchanging the labels for particles 1 and 2 for the helicity and ρ-spin indices it can readily be shown that the contribution of both graphs shown in Fig. 1 are identical.

III. EFFECTIVE EM TWO-BODY $\rho\pi\gamma$ OPERATOR

In a relativistic quasipotential approximation a certain choice is made for the relative energy variable. As a result the current matrix elements simplify to a sixfold integration. The EM operator $\tilde\Gamma_\mu$ is in general a function of the relative energy variables and may lead to a nonphysical singularities depending on the choice made. Following the prescription of Blankenbecler, Sugar and Logunov, Takvlidze[12] (BSLT), where both nucleons are treated on equal footing, we set $p_0=p_0'=0$ in Eqs. (2.17) and (2.18). This has clearly the advantage that no singularities occur in the meson propagators. It implies that the second part of Eq. (2.18) drops out and retardation effects in the meson propagators and strong form factors are neglected.

One additional integration can be carried out explicitly in the current matrix element. Due to rotational invariance the integrand of Eq. (2.21) depends only on the variable $\varphi-\varphi'$ except for a factor $e^{iM\varphi}e^{-iM'\varphi'}$. Hence one azimuthal angle can be done analytically. As a result we are left with a five-dimensional integral, which has to be carried out numerically. The actual reduction of Eq. (2.20) involves lengthy but straightforward algebra. Use has been made of the algebraic program[13] REDUCE to obtain the explicit expressions.

In Ref. 4 it was shown that the so-called static approximation, where certain boost effects are neglected, gives a reasonable description of the relativistic impulse diagram. We employ this to discuss the reliability of the usual nonrelativistic treatment of the MEC contributions. A reduction of Eq. (2.21) can be performed by keeping only the terms of order v/c in the various boost transformations. This amounts to neglecting the Lorentz transformations on k and k' and neglecting the negative energy spinor state components. In the Dirac space, however, we have to replace the boost transformations in Eq. (2.20) by

$$\Lambda^{(1)}(\mathcal{L})V^+_{\lambda_1}(\mathbf{p})\to\sum_{\mu_1}D^{1/2*}_{\lambda_1\mu_1}(\theta_1,\varphi)V^+_{\mu_1}(\tfrac{1}{2}\mathbf{P}+\mathbf{p})\,,$$
$$\Lambda^{(2)}(\mathcal{L})V^+_{\lambda_2}(\mathbf{p})\to\sum_{\mu_2}D^{1/2*}_{-\lambda_2-\mu_2}(\theta_2,\varphi)V^+_{\mu_2}(-\tfrac{1}{2}\mathbf{P}+\mathbf{p})\,, \quad (3.1)$$

where $\theta_1=\theta_{(1/2)\mathbf{P}+\mathbf{p}}-\theta_{\mathbf{p}}$ and $\theta_2=\theta_{-(1/2)\mathbf{P}+\mathbf{p}}-\theta_{\mathbf{p}}$. These replacements are correct up to negative energy contributions, which are of order $(v/c)^2$. The Wigner rotations[14] reflect the fact that the helicities in the Breit frame and in the c.m. frame are not equal, since the helicity is defined as the component of the spin along the direction of momentum. In the nonrelativistic reduction the vertex is defined in the Breit frame and wave functions in the c.m. frame, the Wigner rotations are needed to connect the different helicities. In so doing we obtain as the effective operator

$$\sum_{\mu_1\mu_2}\sum_{\mu_1'\mu_2'}D^{1/2}_{\lambda_1'\mu_1'}(\theta_1',\varphi')D^{1/2}_{-\lambda_2'-\mu_2'}(\theta_2',\varphi')$$
$$\times\Gamma_{n',n,\mu_1',\mu_2',\mu_1,\mu_2}D^{1/2*}_{\lambda_1\mu_1}(\theta_1,\varphi)D^{1/2*}_{-\lambda_2-\mu_2}(\theta_2,\varphi)\,, \quad (3.2)$$

where θ_1' and θ_2' are defined similar to θ_1 and θ_2.

In the usual nonrelativistic estimates of the MEC contributions such as those of Gari and Hyuga[9] and Sitarski, Blunden, and Lomon,[10] a further approximation is made by neglecting recoil corrections, i.e., only the leading order in p/M_N, p'/M_N, and q/M_N are kept in the EM operator. Terms of the form $\mathbf{p}+\mathbf{p}'$ are also neglected. The resulting effective two-body EM current becomes local and as a result facilitates the numerical calculations substantially. If we use the helicity states as defined in Appendix A, Eqs. (A6) and (A7), the expressions for Γ_μ can readily be evaluated in the two-spinor form. They are given by

$$J_0=C_{\rho\pi\gamma}(1+g^T_{\rho NN})\frac{1}{2M_N}$$
$$\times[(\mathbf{k}_\rho\cdot\mathbf{q})\boldsymbol{\sigma}(1)\cdot\mathbf{k}_\rho-(\mathbf{k}_\rho\cdot\mathbf{k}_\rho)\boldsymbol{\sigma}(1)\cdot\mathbf{q}]\frac{1}{2M_N}\boldsymbol{\sigma}(2)\cdot\mathbf{k}_\pi \quad (3.3)$$

and

$$J_+=-C_{\rho\pi\gamma}q(k^1_\rho+ik^2_\rho)\frac{1}{2M_N}\boldsymbol{\sigma}(2)\cdot\mathbf{k}_\pi\,, \quad (3.4)$$

where the Pauli matrices are taken between the rotated Pauli spinors defined in Eq. (A8). The effective operator is defined as in Eq. (3.2). It should be noted that the neglect of recoil corrections yields a current operator J_+ which no longer depends on $g^T_{\rho NN}$, i.e., the tensor term.

We may now compare the results of the EM form factors using both forms of two-body currents. The coupling constants and masses of the mesons are chosen the same as used in the relativistic OBE model,[15] we give them for convenience in Table I. In this model $\Lambda^2=1.5M_N^2$ is used for the cut-off mass of the meson-nucleon form factor. An additional parameter is the $g_{\rho\pi\gamma}$ coupling constant where we take the value found from

TABLE I. Meson masses and coupling constants of the OBE model.

	π	ρ	ω	ε	η	δ
m (MeV)	138.8	763.6	783.4	570.5	548.9	960.8
$(g^V)^2/4\pi$	14.2	0.43	9.92	7.34	3.09	0.33
g^T/g^V		6.8	0			

the decay width of $\rho\to\pi\gamma$. This constant is not well known. Experiments performed by Gobi *et al.*[16] yield a value of $g_{\rho\pi\gamma}=0.38$, while more recent experiments by Berg *et al.*[17] give $g_{\rho\pi\gamma}=0.56$. The value for the coupling constant follows from the decay width, the relation can be found using the coupling Lagrangian in Eq. (2.5), the result is

$$g^2_{\rho\pi\gamma}=\left[\frac{4\pi}{e^2}\right]\frac{24\Gamma(\rho\to\pi\gamma)}{m_\rho(1-m_\pi^2/m_\rho^2)^3}\ . \tag{3.5}$$

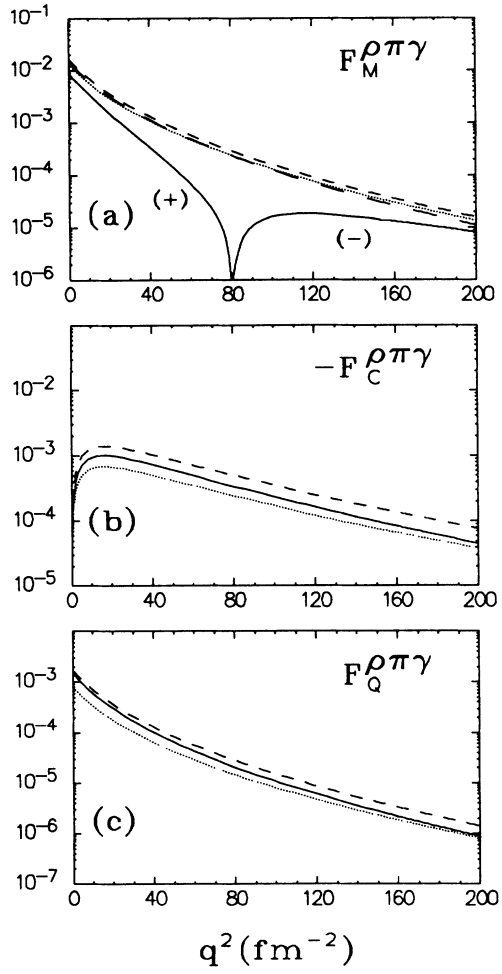

FIG. 2. The $\rho\pi\gamma$ MEC form factors for the RSC wave function. The dashed line is the result with the nonrelativistic two-body EM operator the solid line with the full EM operator, and the long dashed line the γ^0 contribution as defined in Eq. (2.18). For comparison the Gari and Hyuga (Ref. 9) results are shown (dotted line).

However, nothing can be said about the sign of the coupling constant. In the calculations we take $g_{\rho\pi\gamma}$ to be positive. In Fig. 2 the calculated results of $F_C^{\rho\pi\gamma}$, $F_Q^{\rho\pi\gamma}$, and $F_M^{\rho\pi\gamma}$, together with their sign, are shown for the case of the Reid soft core (RSC) wave function. The solid lines give the results with the full effective two-body EM operator used and $g_{\rho\pi\gamma}=0.56$. The dashed lines corresponds to the results for the usual localized nonrelativistic EM operator, i.e., retaining the leading-order term in p/M_N, p'/M_N, and q/M_N. Effects of the higher-order terms in p/M_N, p'/M_N, and q/M_N are large even at low q^2. In $F_C^{\rho\pi\gamma}$ and $F_Q^{\rho\pi\gamma}$ the difference at $q^2=0$ is about 20%, but it is much greater in the magnetic form factor $F_M^{\rho\pi\gamma}$. The latter is due to the tensor term which is absent in the usual nonrelativistic current. In Fig. 2(a) we show the nonlocal result without the tensor part of the contribution (long dashed). The difference is now of the same order as in the electric form factors. Inspection of the integral shows that for $|\mathbf{p}-\mathbf{p}'|\sim 1$ GeV/c there are still important contributions. In this momentum region the tensor term is of the same order as the γ^0 terms in Eq. (2.18). However these contributions have opposite sign and therefore there is a large cancellation. This large momentum dependence also explains the sizable effects of the choice of the monopole form factors as found by Gari and Hyuga.[9] Their results are well reproduced with our momentum space program. For comparison they are also shown in the figures (dotted lines). In addition to different strengths of the OBE parameters a value of $g_{\rho\pi\gamma}=0.38$ was used in their calculations.

IV. RELATIVISTIC ANALYSIS

With the effective two-body EM currents as given in the previous section we have carried out a quasipotential calculation using the relativistic OBE model of Ref. 15. We have used in our study the symmetric choice of BSLT for the quasipotential Green's function. This is obtained by replacing the scalar part

$$\begin{aligned}S_0=&[(\tfrac{1}{2}P_{\text{c.m.}}-k)^2-m^2+i\epsilon]^{-1}\\&\times[(\tfrac{1}{2}P_{\text{c.m.}}+k)^2-m^2+i\epsilon]^{-1}\end{aligned} \tag{4.1}$$

of the two nucleon propagator in Eq. (2.3) and Eq. (2.12) by

$$S_0=i\pi\delta(k_0)\frac{1}{(E+E_k)^2(E_k-E-i\varepsilon)}\ , \tag{4.2}$$

where $E=\frac{1}{2}P_{0_{\text{c.m.}}}$, $E_k=\sqrt{\mathbf{k}^2+m^2}$. In the BSLT approximation the two nucleon propagator becomes diagonal in the total ρ-spin representation. Using Eq. (4.2) we get

$$\begin{aligned}S_{++}(k,P_{\text{c.m.}})&=\tfrac{1}{2}\frac{1}{E_k-E-i\varepsilon}\ ,\\S_{--}(k,P_{\text{c.m.}})&=\tfrac{1}{2}\frac{E_k-E}{(E_k+E)^2}\ ,\\S_{ee}(k,P_{\text{c.m.}})&=S_{oo}(k,P_{\text{c.m.}})=-\tfrac{1}{2}\frac{1}{E_k+E}\ .\end{aligned} \tag{4.3}$$

The quasipotential two nucleon propagator can be written in the more compact form

$$S_2^{\mathrm{BSLT}}(k,P_{\mathrm{c.m.}})=H(k)S^{(1)}(\tfrac{1}{2}P_{\mathrm{c.m.}}+k)S^{(2)}(\tfrac{1}{2}P_{\mathrm{c.m.}}-k)\ , \tag{4.4}$$

where $H(k)=E_k-E$. In this OBE model the interaction V in Eq. (2.4) is described by exchange of π, ρ, ω, ε, η, and δ mesons. To calculate the deuteron vertex function the quasipotential equations are solved[18] with the BSLT prescription for the two-nucleon Green's function. In Fig. 3 are shown the EM form factors for the $\rho\pi\gamma$ graph using the two-body EM operators as described in the previous section. For the nonrelativistic (local) two-body EM current the results are shown for both RSC (dotted) and BSLT (dashed) wave function. From this we see that there is a large wave function dependence.

We have examined in some detail where this large sensitivity comes from. The major reason is that there are substantial contributions from the momentum range $0.5\sim1.0$ GeV/c in the loop integrals where the various deuteron vertex functions differ significantly (see Fig. 4). Also the D-wave components contribute in an important way, its magnitude being very different in the two vertex functions because of their different D-state probability. Moreover, a large cancellation takes place between the S and D wave contributions, so differences in the wave functions become more enhanced.

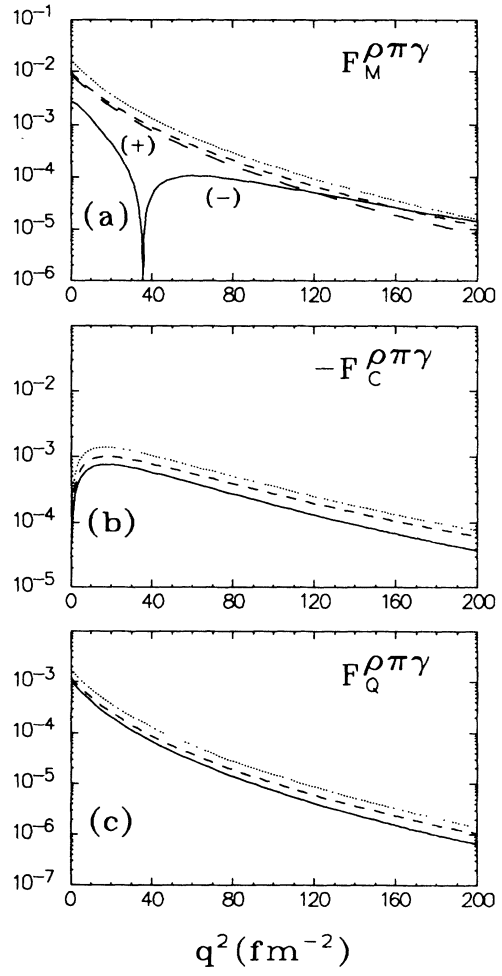

FIG. 3. The $\rho\pi\gamma$ MEC form factors for the BSLT wave function. The dashed line is the result with the nonrelativistic two-body EM operator, the solid line with the full EM operator, and the long dashed line the γ^0 contribution as defined in Eq. (2.18). For comparison the nonrelativistic result with the RSC wave function is also shown (dotted line).

The solid lines give the results with the full effective two-body EM operator and the BSLT wave function. Effects of the higher-order terms in p/M_N, p'/M_N, and q/M_N are in $F_C^{\rho\pi\gamma}$ and $F_Q^{\rho\pi\gamma}$ of the same order as when a RSC wave function is used, see Fig. 2. The results for the magnetic form factor has however a dip at much lower q^2 as found for the result with RSC wave function (Fig. 2). Inspection shows that this dip is mainly due to large cancellation between the γ^0 contribution and the tensor contribution, as we discussed already in Sec. III. Comparison between the γ^0 contributions of Fig. 2(a) and Fig. 3(a) (long dashed) shows similar wave function dependence as found earlier. As a consequence of the cancellation the magnetic form factor is very wave function dependent.

The boost corrections to the static approximation of the two-body EM current can be calculated. They are shown in Fig. 5. For comparison the static results (dotted) with the full effective operator are shown. The dashed line is the result with boost effects taken into account, while the result with the negative energy state contributions (with boost effects) are given by the solid line. As can be seen from the figure, these corrections are small.

We now turn to the discussion of the $\omega\varepsilon\gamma$ MEC contribution. The calculation is similar to the $\rho\pi\gamma$ graph, using the procedure as described in Sec. II. For the Lagrangians we take

$$\begin{aligned} L_{\varepsilon NN}&=g_{\varepsilon NN}\bar{u}(p)\varepsilon u(p')\ ,\\ L_{\omega NN}&=g_{\omega NN}\bar{u}(p)\gamma_\mu\omega^\mu u(p')\ ,\\ L_{\omega\varepsilon\gamma}&=-\frac{eg_{\omega\varepsilon\gamma}}{m_\omega}F_{\alpha\beta}\omega^\alpha\partial^\beta\varepsilon\ , \end{aligned} \tag{4.5}$$

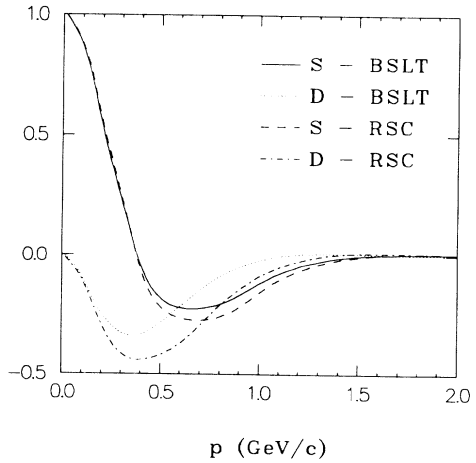

FIG. 4. The S- and D-wave components of the deuteron vertex function.

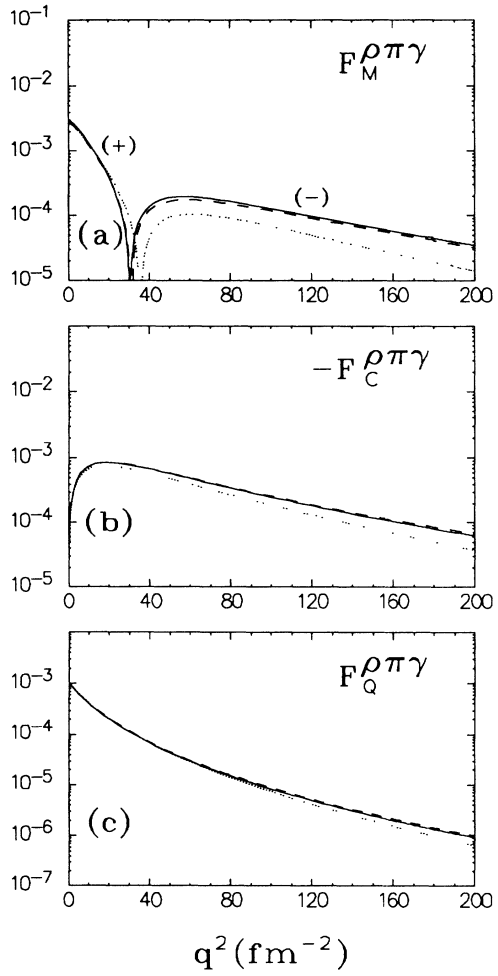

FIG. 5. The $\rho\pi\gamma$ MEC form factors. The solid line is with boost effects and negative energy states included, while the dashed line is without negative energy states. For comparison the dotted line is with the full two-body EM operator.

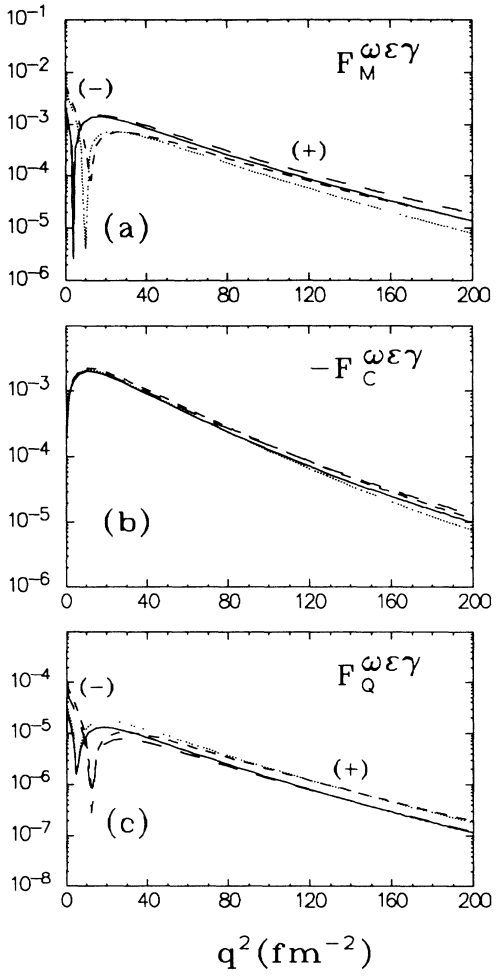

FIG. 6. The $\omega\varepsilon\gamma$ MEC form factors. The solid line represents the results with the nonlocal EM operator and the dashed line the results with the nonrelativistic EM operator, both for the BSLT wave function. Using the RSC wave function the results are shown as the dotted and long dashed lines.

which gives for the charge operator

$$J_0(k_\varepsilon,k_\omega)=-C_{\omega\varepsilon\gamma}\gamma_0(1)q\cdot k_\varepsilon \tag{4.6}$$

and for the current operator

$$J_+(k_\varepsilon,k_\omega)=C_{\omega\varepsilon\gamma}\left[[\gamma^1(1)+i\gamma^2(1)]q\cdot k_\varepsilon - \left[\not{q}(1)-\frac{k_\omega(1)\mathbf{q}^2}{m_\omega^2}\right](k_\varepsilon^1+ik_\varepsilon^2)\right], \tag{4.7}$$

where $C_{\omega\varepsilon\gamma}$ is defined similar to $C_{\rho\pi\gamma}$ and all retardation terms are left out. Because of the $\omega\varepsilon\gamma$ coupling, this current is gauge invariant. No experiments exist to determine the $\omega\varepsilon\gamma$ coupling constant. To get an estimate of it various theoretical models have been studied in the literature. Using a relativistic quark model Chemtob, Moniz, and Rho[11] arrive at the result $g_{\omega\varepsilon\gamma}\approx -g_{\rho\pi\gamma}$. More recently using a quantum hadron dynamical (QHD) model the effective $\omega\varepsilon\gamma$ coupling constant has been deduced by Horowitz[7] in the random-phase approximation (RPA). In this analysis $g_{\omega\varepsilon\gamma}$ can be expressed in terms of $g_{\varepsilon NN}$ and $g_{\omega NN}$, resulting in a value of $|g_{\omega\varepsilon\gamma}|=1$. If our relativistic OBE model parameters are used we get $|g_{\omega\varepsilon\gamma}|=1.6$. An experimental upper limit can be set by the decay $\omega\to 2\pi^0\gamma$ and by the condition $\Gamma(\omega\to\varepsilon\gamma)<3\Gamma(\omega\to 2\pi^0\gamma)$, where $\Gamma(\omega\to 2\pi^0\gamma)<0.14$ MeV.[19] The Lagrangian for the $\omega\varepsilon\gamma$ coupling gives a similar relation between the decay width and the coupling constant as for $\rho\pi\gamma$. With the above upper limit for $\omega\to 2\pi^0\gamma$ we get $|g_{\omega\varepsilon\gamma}|<2.4$.

Since the boost effects and the negative energy contributions appear to be small, we have only analyzed the $\omega\varepsilon\gamma$ graph in the static approximation. In Fig. 6 the results are shown for the case that $g_{\omega\varepsilon\gamma}=-0.56$ as obtained from the relativistic quark model and the value of the $\rho\pi\gamma$ coupling constant. The S-wave contribution is the most important contribution to the electric matrix elements resulting in a very small wave function dependence of $F_C^{\omega\varepsilon\gamma}$. From the figure we see that only for the

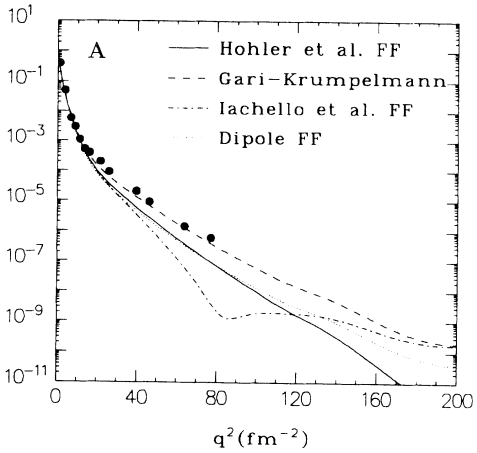

FIG. 7 The electron form factor for the OBE model of the deuteron in IA with various choices of one nucleon form factors. The data are from Ref. 1.

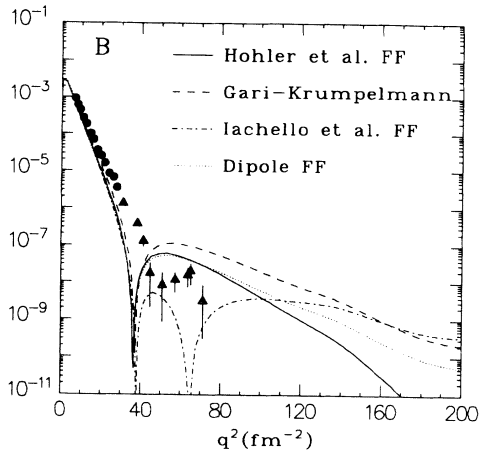

FIG. 8. The magnetic form factor of the deuteron in IA with various choices of one nucleon form factors. The data labeled by ● and Δ are from Refs. 2 and 3.

quadrupole form factor, the recoil corrections make a sizable difference, while there is a clear wave function dependence in $F_M^{\omega\varepsilon\gamma}$. Moreover, the quadrupole and magnetic form factors have a dip at moderate momentum transfer. The one in $F_Q^{\omega\varepsilon\gamma}$ is due to a change of sign in the D-wave contribution, whereas the dip in the magnetic form factor is caused by an interplay between the various contributions including the S-wave matrix elements.

In addition to the $\rho\pi\gamma$ and $\omega\varepsilon\gamma$ MEC there are more isoscalar currents. If the mesons in the OBE model are used, there are three more isoscalar MEC's: $\omega\eta\gamma$, $\rho\delta\gamma$, and $\delta\pi\gamma$. The δ is a scalar meson. Therefore the $\delta\pi\gamma$ coupling has the form $\varepsilon_{\mu\nu\alpha\beta}F^{\mu\nu}k_\delta^\alpha k_\pi^\beta$. Since at the $\delta\pi\gamma$ vertex we have $k_\delta+q=k_\pi$, due to the antisymmetric Levi-Civita tensor this graph does not give a contribution. The $\rho\delta\gamma$ has roughly the same structure as the $\omega\varepsilon\gamma$ MEC. The differences are only in the isospin structure and the tensor part of the ρNN coupling. If we compare the couplings of the mesons to the nucleons (see Table I) for both currents we see that that $\rho\delta\gamma$ current is much smaller and can be neglected. This is not the case for the $\omega\eta\gamma$ MEC, which structure can be compared with the $\rho\pi\gamma$ MEC. Calculations show that the electric form factors are negligibly small, but that the magnetic form factor is a factor 2 or 3 smaller as the $\omega\varepsilon\gamma$ form factor. In this calculation we used a value 0.56 for the $\omega\eta\gamma$ coupling (in that case the $\omega\eta\gamma$ contribution to the magnetic form factor is of opposite sign as the $\omega\varepsilon\gamma$ contribution). Experimental upper limit to this value is set by Andrews *et al.*[20] Their highest value $\Gamma(\omega\to\eta\gamma)=29\pm7$ keV gives with a relation similar to the one used for the $\rho\pi\gamma$ coupling a value $|g_{\omega\eta\gamma}|=0.96$.

V. DEUTERON EM FORM FACTORS

Within the Bethe-Salpeter (BS) and the relativistic quasipotential formalism an extensive study of relativistic effects has been made previously[4,5] for the electric and magnetic form factors in the impulse approximation (IA). Use was made of dipole form factors for the one nucleon EM form factors. Various other parametrizations of these form factors have in the meantime become available. In particular, the behavior of the neutron form factor can differ substantially at higher momentum transfer. We have studied in the relativistic OBE model the sensitivity of the deuteron form factors on the choice of these parametrizations. In Figs. 7 and 8 are shown the effects of the Gari-Krümpelmann[21] and the Höhler *et al.*[22] form factors on the IA. For the dipole form factors, we use the phenomenological dipole form factors

$$F_1^S(q^2)=\Delta(q^2)\left[1+\frac{-0.12}{1-\tau}\right],$$
$$F_2^S(q^2)=\Delta(q^2)\left[\frac{-0.12}{1-\tau}\right], \tag{5.1}$$

where $\Delta(q^2)=(1-q^2/\Lambda)^{-2}$, $\tau=q^2/(4M_N^2)$, and $\Lambda=0.71$ GeV.[2] We also show the results for the dipole form factors of Iachello, Jackson, and Landé.[23]

In our calculations we use the BSLT prescription for both the initial and final states. It should be noted, that strictly speaking both wave functions cannot have at the same time $k_0=0$, because of momentum conservation.[24] To deduce a possible form in this approximation for the IA, we start with the deuteron current in the c.m. frame,

$$\langle P',M'|J_\mu^{\mathrm{IA}}|P,M\rangle=\frac{ie}{8\pi^3M_D}\int d^4k\,\tilde{\Phi}_D^{(M')}(k';P'_{\mathrm{c.m.}})S^{(1)}(\tfrac{1}{2}P'_{\mathrm{c.m.}}+k')\Lambda^{-1}(\mathcal{L}')\Gamma_\mu^{(1)}(q)\Lambda(\mathcal{L})S_2(k,P_{\mathrm{c.m.}})\Phi_D^{(M)}(k;P_{\mathrm{c.m.}})\,. \tag{5.2}$$

In the reduction as studied in Ref. 24 only the positive energy intermediate states were considered. Both k_0 and k_0' are set to zero in the integrand and the scalar parts of the propagators are replaced by $i\pi S_{++}(k',P'_{\text{c.m.}})S_{++}(k,P_{\text{c.m.}})$. In this approximation the deuteron current can be written in the form

$$\langle P',M'|J_\mu^{\text{IA}}|P,M\rangle=\frac{-e}{8\pi^2 M_D}\int d^3k\,\tilde{\Phi}_D^{(M')}(\mathbf{k}';P'_{\text{c.m.}})S_{++}(k',P'_{\text{c.m.}})\Lambda_+^{(1)}(\mathbf{k}')$$
$$\times\Lambda^{-1}(\mathcal{L}')\Gamma_\mu^{(1)}(q)\Lambda(\mathcal{L})\Lambda_+^{(1)}(\mathbf{k})\Lambda_+^{(2)}(\mathbf{k})S_{++}(k,P_{\text{c.m.}})\Phi_D^{(m)}(\mathbf{k};P_{\text{c.m.}})\ . \tag{5.3}$$

The normalization condition can be verified by letting $q\to 0$ in Eq. (5.3). In the BSLT quasipotential framework, this condition takes instead of Eq. (2.4) the form

$$2P_\mu\delta_{M,M'}=\frac{-1}{4\pi^2}\int d^3k\,\tilde{\Phi}_D^{(M)}(\mathbf{k};P)\left[\frac{\partial}{\partial P_\mu}S_2^{\text{BSLT}}(k,P)\right]_{P^2=M_D^2}\Phi_D^{(M')}(\mathbf{k};P)\ . \tag{5.4}$$

In the special case that we only keep the positive energy states in the current matrix elements, we have for $\mu=0$ in the limit $q\to 0$

$$\langle P',M'|J_0^{\text{IA}}|P,M\rangle=\frac{-e}{8\pi^2 M_D}\int d^3k\,\tilde{\Phi}_D^{(M')}(\mathbf{k};P_{\text{c.m.}})S_{++}(k,P_{\text{c.m.}})\Lambda_+^{(1)}(\mathbf{k})$$
$$\times\gamma_0^{(1)}\Lambda_+^{(1)}(\mathbf{k})\Lambda_+^{(2)}(\mathbf{k})S_{++}(k,P_{\text{c.m.}})\Phi_D^{(M)}(\mathbf{k};P_{\text{c.m.}})\ . \tag{5.5}$$

It can easily be verified that the normalization condition Eq. (5.4) indeed holds in this approximation.

We generalize the prescription Eq. (5.3) for the deuteron current to include also the negative intermediate states,

$$\langle P',M'|J_\mu^{\text{IA}}|P,M\rangle=\frac{-e}{8\pi^2 M_D}\int d^3k\,\tilde{\Phi}_D^{(M')}(\mathbf{k}';P'_{\text{c.m.}})S_2^{\text{BSLT}}(k',P'_{\text{c.m.}})$$
$$\times\gamma_0^{(2)}\Lambda^{-1}(\mathcal{L}')\Gamma_\mu^{(1)}(q)\Lambda(\mathcal{L})S_2^{\text{BSLT}}(k,P_{\text{c.m.}})\Phi_D^{(M)}(\mathbf{k};P_{\text{c.m.}})\ . \tag{5.6}$$

This deuteron current gives the same result as Eq. (5.3) if we keep only the positive energy states. Comparing Eq. (5.4) with Eq. (5.6) we find that except for the $(--)$ states, the normalization condition holds. For these states a correction of the form $-4E_k^2/(E+E_k)^4\Lambda_{--}\gamma_0^{(1)}\gamma_0^{(2)}\Lambda_{--}$ has to be added to the charge operator in order to satisfy Eq. (5.4). Explicit estimates of this correction show that it is very small and therefore it can be safely neglected. In the whole momentum square region 0–200 fm^{-2} its correction to the charge form factor is below 1%. Only at very high momentum transfer ($q^2>120$ fm^{-2}) the correction is somewhat ($<5\%$) higher for the quadrupole form factor of the deuteron.

For the electric form factor the results with the Gari-Krümpelmann form factors are in close agreement with the experiment, whereas the calculated magnetic form factors are too low in magnitude for moderately large momentum transfer, while the dip occurs at too low q^2. In Figs. 9 and 10 are shown the OBE results with the $\rho\pi\gamma$ (boosts and negative energy states included) and the $\omega\varepsilon\gamma$ graphs included. Use is made of Höhler *et al.* form

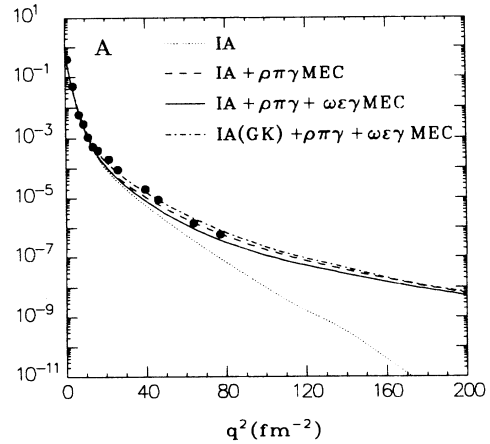

FIG. 9. The electric form factor of the deuteron, including the MEC contribution, with Höhler *et al.* form factors and BSLT wave function. Dotted-dashed line is with Gari-Krümpelmann nucleon form factors.

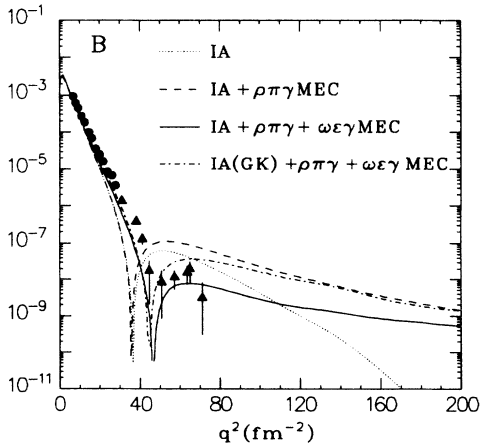

FIG. 10. The same as Fig. 9, but for the magnetic form factor.

factors. The IA results are close to those found in the Bethe-Salpeter calculations.[4] As compared to the experimental data including the MEC calculations clearly yield a significant improvement both in the A and B form factors. The $\rho\pi\gamma$ contribution brings the result for A in better agreement with the data. In particular, the $\omega\varepsilon\gamma$ contribution causes the dip in the magnetic form factor to shift to higher momentum transfer to roughly the experimentally found value. If the one nucleon form factors of Gari and Krümpelmann are used, the overall agreement with experiment can be qualified as better than with the Höhler *et al.* form factors. However it should be noted that the results at high momentum transfer are very sensitive to the $\omega\varepsilon\gamma$ coupling constant. If, for example, the value predicted by the RPA formalism[7] is used, the dip in B disappears completely, while the results for A are lowered, yielding a significant deviation from the experiment. The sign of the $g_{\rho\pi\gamma}$ coupling constant is also very important. The full result for the electric form factor A (Fig. 9) is in better agreement with the data if a positive value is used. A negative value would bring the total result even below the IA result.

In Figs. 11 and 12 are shown the nonrelativistic results for the RSC wave function and using again the Höhler *et al.* form factors. In this case the $\rho\pi\gamma$ MEC contribution is considerably larger if one uses the nonrelativistic approximation for the current operator. As a result there is an overshoot of the electric form factor and the dip in the magnetic form factor completely disappears. Using the full (nonlocal) two-body current operator for the MEC graphs however leads to a strong weakening of the $\rho\pi\gamma$ contribution, resulting in good agreement with the data. Moreover, from the figures we see that the RSC wave function IA results are in better agreement with the magnetic form factor data than those of the BSLT wave function. This can be ascribed to the larger D-state probability of the RSC wave function. The above effect is also found in the calculations of Chung *et al.*,[25] where the best results regarding the data are found with the AV14 potential, having the highest D-state probability of the potentials considered by them.

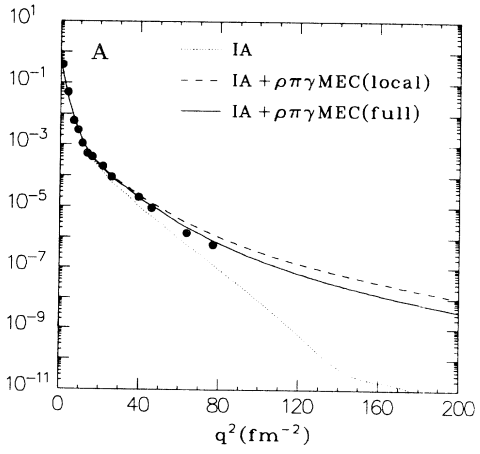

FIG. 11. The electric form factor of the deuteron, including the $\rho\pi\gamma$ MEC, with Höhler *et al.* nucleon form factors and RSC wave function.

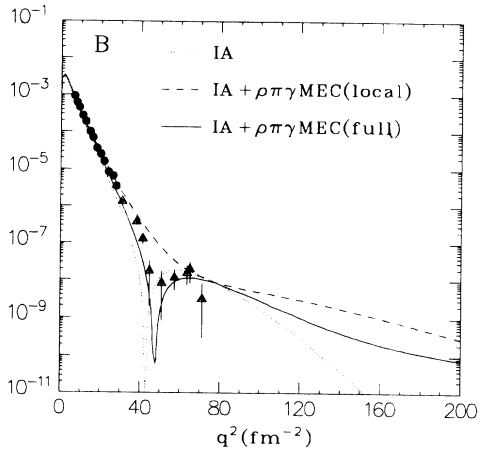

FIG. 12. The same as Fig. 11, but for the magnetic form factor.

Recently new results of precision measurements[26] of the electric form factor A became available at low momentum transfer. In Fig. 13 we compare our results with these experiments. For momentum transfer $q^2 > 10$ fm^{-2} the IA with Höhler *et al.* form factors and BSLT wave function is below the data. Inclusion of the MEC's improves the result but the contribution of the MEC's is small. If use is made of Gari-Krümpelmann form factors the data can be described. This same result can be achieved if a RSC wave function is used with Höhler *et al.* one nucleon form factors. These results show that for low momentum transfer the MEC's are negligible for the electric form factor.

Low momentum transfer study of the form factors gives us information about the quadrupole moment Q_d and the magnetic moment μ_d of the deuteron (see Appendix B). In Tables II and III we show our calculations of these moments for BSLT and RSC wave function and Höhler *et al.* form factors. A very large wave function dependence is seen in the magnetic moment and a some-

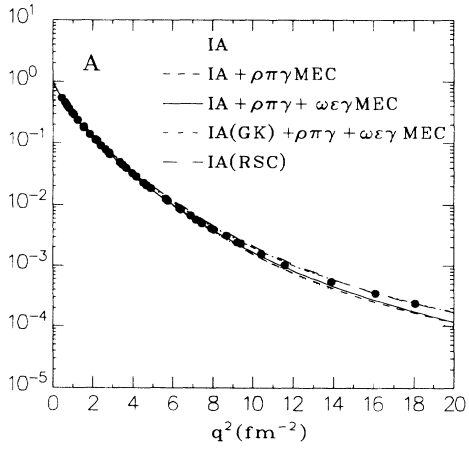

FIG. 13. The electric form factor A for low momentum transfer, data from Ref. 26.

TABLE II. Results for the magnetic moment of the deuteron for the IA and the MEC's included. Experimental value $\mu_d = 0.857\,406 \pm 0.000\,001$.

	IA	$\rho\pi\gamma(10^{-2})$ local	$\rho\pi\gamma(10^{-2})$ full	$\rho\pi\gamma(10^{-2})$ complete	$\omega\varepsilon\gamma(10^{-2})$ local	$\omega\varepsilon\gamma(10^{-2})$ full
BSLT	0.858	0.483	0.140	0.154	−0.123	−0.110
RSC	0.837	0.840	0.444		−0.289	−0.228

what smaller effect in the quadrupole moment. As already discussed in Secs. III and IV this is due to large contributions of high momenta in the integral. This explains also the large effect if no expansion is made in the EM operator (full result). Inclusions of boost effects and negative energy state contributions (complete result) only give small effects, 10% and 3%, for, respectively, the magnetic moment and quadrupole moment as compared to the full calculation. The effect for the magnetic moment is totally due to the negative energy states. If the BSLT wave function is used, the IA result for the magnetic moment is close to the experimental value. The RSC result is much lower. This tendency, although not so pronounced, is also found by Chung, Keister, and Coester,[27] where wave functions with a P_D of about 5% give the best result. In the OBE model the BSLT wave function has $P_D = 4.5\%$. Other choices for the one nucleon form factors show a negligible dependence on these form factors. Inclusion of the $\rho\pi\gamma$ and $\omega\varepsilon\gamma$ MEC do not change the IA results, also due to the cancellation of the contributions. For the quadrupole moment, the IA is for both wave functions below the experimental value. Only the $\rho\pi\gamma$ MEC gives a small contribution (0.4%). However, the total result $Q_d = 0.270$ is still below the experimental value.

Finally in Fig. 14 is shown the calculated tensor polarization of the deuteron. The relativistic IA result[29] is close to the nonrelativistic RSC prediction, in agreement with Frankfurt *et al.*,[30] but in contrast to the finding of Dymarz and Khanna.[31] The first dip in the relativistic IA result is due to a dip in F_C and the second one is due to a dip in the quadrupole form factor F_Q. In a nonrelativistic RSC calculation the dip in F_Q is for lower momentum while also a second dip in F_C occurs. As a result the second dip in t_{20} is shifted to higher momentum transfer. Inclusion of the MEC contributions do not have an effect at low momentum transfer, where the agreement with the existing experiments is good. At higher momentum transfer the MEC corrections are significant, thereby shifting the zero in t_{20} to higher momentum transfer. In this case use of the Höhler *et al.* or the Gari-Krümpelmann form factors does not lead to large differences, except at very large momentum transfer.

VI. CONCLUDING REMARKS

We have studied the $\rho\pi\gamma$ graph in the relativistic OBE model. In the usual calculations an expansion in p/M_N, p'/M_N, and q/M_N of the current operator is made, keeping only the leading terms. We have shown here that such an approximation is not reliable and the full EM operator is needed. In the analysis we have assumed in the two-body EM current that the relative energy variable is zero. To get some idea about the sensitivity on the specific choice of the relative energy variable we have considered also the case that the EM operator is calculated assuming the nucleons on mass shell. A problem is the second part of the current in Eq. (2.18) proportional to k_π^0. Because of the Levi-Civita tensor [Eq. (2.8)] k_π^0 can also be replaced by k_ρ^0. Energy momentum conservation forbids to put both nucleons on mass shell. If we force the nucleons independently on mass shell, the relative energies of the ρ and π mesons are equal but of opposite sign. We therefore neglect the term in the current operator proportional to the relative energy. In Fig. 15 we show the results where still the retardation effects in the meson propagators and form factors are neglected. From this we see that the largest sensitivity of the $\rho\pi\gamma$ graph is found for the magnetic form factor. However the recoil corrections are such that the contributions at large momentum transfer are considerably reduced. If retardation effects are taken into account the results are very similar to the results if using the BSLT constraint. The effects in both electric and magnetic form factors are comparable to the effects found for the electric form factors in Fig. 15.

Boost effects and contributions from negative energy states have been studied in the relativistic OBE model with a BSLT wave function, showing that they essentially

TABLE III. Results for the quadrupole moment of the deuteron for the IA and the MEC's included. Experimental value $Q_d = 0.2860 \pm 0.000\,15$.

	IA	$\rho\pi\gamma(10^{-2})$ local	$\rho\pi\gamma(10^{-2})$ full	$\rho\pi\gamma(10^{-2})$ complete	$\omega\varepsilon\gamma(10^{-4})$ local	$\omega\varepsilon\gamma(10^{-4})$ full
BSLT	0.269	0.121	0.107	0.104	−0.668	−0.307
RSC	0.279	0.174	0.153		−0.913	−0.396

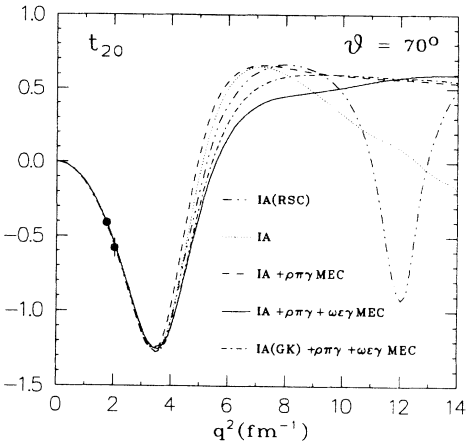

FIG. 14. The deuteron tensor polarization t_{20} for the relativistic OBE wave function with Höhler *et al.* one nucleon form factors. The data are from Ref. 28.

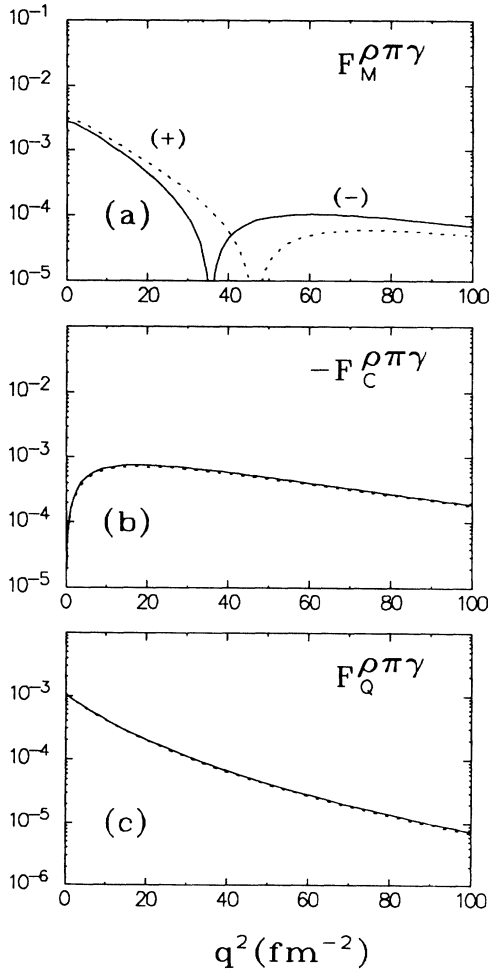

FIG. 15. The $\rho\pi\gamma$ MEC form factors. The solid line is the result with zero relative energy and the dashed line the on-mass-shell case. The full EM operator and the BSLT wave function are used here.

can be neglected. Comparison of static results in this model and of static results with a RSC wave function show a large wave function dependence. The $\rho\pi\gamma$ graph depends sensitively on the *D*-wave component of the deuteron wave function. The *D-S*, *S-D*, and *D-D* matrix elements are of the same order as the *S-S* matrix elements, but there are large cancellations between the different matrix elements.

Using the deuteron wave function as obtained from the relativistic OBE model we have found that the agreement with the experimental data is rather poor when we only take the IA contribution into account. In particular, the calculated magnetic form factor is too low, even for the Gari-Krümpelmann nucleon form factors. Inclusion of the $\rho\pi\gamma$ and $\omega\varepsilon\gamma$ MEC contributions improves considerably the calculated deuteron EM form factors. In view of the substantial reduction of the $\rho\pi\gamma$ graph due to recoil corrections, the $\omega\varepsilon\gamma$ contribution becomes more important at high momentum transfer, moving both the elastic and magnetic form factors in the proper direction.

In the relativistic model studied here we find, that the MEC contributions are needed to account for the experimentally found elastic EM deuteron form factors. It should be emphasized that the calculations are sensitive to the choice of the various EM coupling constants such as the $g_{\omega\varepsilon\gamma}$, which are not very well known at present. Even a small contribution like from the $\omega\eta\gamma$ MEC is very important in the dip region of the magnetic form factor of the deuteron. Moreover, the short-range character of the MEC graphs leads to considerable dependence on the choice of the strong form factors in the πNN and ρNN vertices.

ACKNOWLEDGMENTS

This work was partially financially supported by de Stichting voor Fundamenteel Onderzoek der Materie (FOM), which is sponsored by Nederlandse Organisatie voor Wetenschappelijk Onderzoek (NWO).

APPENDIX A

In the calculation of the current matrix elements we use the helicity and ρ-spin formalism in the Dirac spinors, following Kubis[32] and Fleischer,[33] together with the convention of Bjorken and Drell.[34] We start with the spinors

$$u_\lambda(p)=N_p\begin{bmatrix}1\\ \dfrac{2\lambda p}{E_p+M}\end{bmatrix}\chi_\lambda\ ,$$
$$w_\lambda(p)=N_p\begin{bmatrix}\dfrac{-2\lambda p}{E_p+M}\\ 1\end{bmatrix}\chi_\lambda\ , \tag{A1}$$

which are the positive and negative energy solutions of the Dirac equation. χ_λ are the Pauli spinors with helicity λ and with normalization $N_p=\sqrt{(E_p+M_N)/2E_p}$. In case of two particles we define for particle 1

$$U_{\lambda_1}(p)=u_{\lambda_1}(p)\ ,$$
$$W_{\lambda_1}(p)=(-1)^{(1/2)+\lambda_1}\Lambda_{31}(\pi)w_{\lambda_1}(p) \tag{A2}$$

and for particle 2

$$U_{\lambda_2}(p)=(-1)^{(1/2)-\lambda_2}\Lambda_{31}(\pi)u_{\lambda_2}(p)\ ,$$
$$W_{\lambda_2}(p)=w_{\lambda_2}(p)\ , \tag{A3}$$

where $\Lambda_{ab}(\alpha)$ is a rotation in the plane defined by the a axis and the b axis:

$$\Lambda_{ab}(\alpha)=\cos\alpha/2+\gamma^a\gamma^b\sin\alpha/2\ . \tag{A4}$$

In ρ-spin notation we define $V^\rho_\lambda(\mathbf{p})$, with $V^+_\lambda(\mathbf{p})=U_\lambda(\mathbf{p})$ and $V^-_\lambda(\mathbf{p})=W_\lambda(\mathbf{p})$. The rotated spinors are defined by

$$V^\rho_\lambda(\mathbf{p})=\Lambda_{12}(\varphi)\Lambda_{31}(\theta)\Lambda^{-1}_{12}(\varphi)V^\rho_\lambda(p)\ . \tag{A5}$$

For particle 1 we have

$$V^+_{\lambda_1}(\mathbf{p})=N_p\begin{pmatrix}1\\ \dfrac{\boldsymbol{\sigma}\cdot\mathbf{p}}{E_p+M}\end{pmatrix}\chi_{\lambda_1}(\theta,\varphi)\ ,$$
$$V^-_{\lambda_1}(\mathbf{p})=N_p\begin{pmatrix}\dfrac{-\boldsymbol{\sigma}\cdot\mathbf{p}}{E_p+M}\\ 1\end{pmatrix}\chi_{\lambda_1}(\theta,\varphi) \tag{A6}$$

and for particle 2

$$V^+_{\lambda_2}(\mathbf{p})=N_p\begin{pmatrix}1\\ \dfrac{-\boldsymbol{\sigma}\cdot\mathbf{p}}{E_p+M}\end{pmatrix}\chi_{-\lambda_2}(\theta,\varphi)\ ,$$
$$V^-_{\lambda_2}(\mathbf{p})=N_p\begin{pmatrix}\dfrac{\boldsymbol{\sigma}\cdot\mathbf{p}}{E_p+M}\\ 1\end{pmatrix}\chi_{-\lambda_2}(\theta,\varphi)\ , \tag{A7}$$

where $\chi_\lambda(\theta,\varphi)$ are the rotated Pauli spinors,

$$\chi_{1/2}(\theta,\varphi)=\begin{pmatrix}\cos\theta/2\\ e^{i\varphi}\sin\theta/2\end{pmatrix}\ ,$$
$$\chi_{-1/2}(\theta,\varphi)=\begin{pmatrix}-e^{-i\varphi}\sin\theta/2\\ \cos\theta/2\end{pmatrix}\ . \tag{A8}$$

Defined in this way the spinors are normalized as

$$V^{\rho\dagger}_\lambda(\mathbf{p})V^{\rho'}_{\lambda'}(\mathbf{p})=\delta_{\rho\rho'}\delta_{\lambda\lambda'} \tag{A9}$$

and form a complete set

$$\sum_{\rho\lambda}V^\rho_\lambda(\mathbf{p})V^{\rho\dagger}_\lambda(\mathbf{p})=\sum_\rho\Lambda_\rho(\mathbf{p})\gamma_0=1\ , \tag{A10}$$

where $\Lambda_\rho(\mathbf{p})=\sum_\lambda V^\rho_\lambda(\mathbf{p})\bar V^\rho_\lambda(\mathbf{p})$ are the ρ-spin projection operators. These spinors can be used to expand the nucleon propagators

$$S^{(i)}(p)=(\not p-M_N+i\epsilon)^{-1}$$
$$=\frac{\sum_{\lambda_i}V^+_{\lambda_i}(\mathbf{p})\bar V^+_{\lambda_i}(\mathbf{p})}{p_0-E_p-i\epsilon}+\frac{\sum_{\lambda_i}V^-_{\lambda_i}(\mathbf{p})\bar V^-_{\lambda_i}(\mathbf{p})}{p_0+E_p-i\epsilon}\ , \tag{A11}$$

where $i=1,2$. This expression can also be written in the form $S^{(i)}(p)=\Lambda^i_+(\mathbf{p})S_+(p)+\Lambda^i_-(\mathbf{p})S_-(p)$, where $S_\rho(p)$ are the scalar parts of the propagators.

The deuteron vertex function $\Phi^{(M)}_D(p;P_{\text{c.m.}})$ satisfies the homogeneous Bethe-Salpeter equation (BSE). Using the helicity states basis we can define in the two nucleon c.m. frame

$$\phi^{(M)}(p,a)=\bar V^{\rho_1}_{\lambda_1}(\mathbf{p})\bar V^{\rho_2}_{\lambda_2}(\mathbf{p})\Phi^{(M)}_D(p;P_{\text{c.m.}})\ , \tag{A12}$$

where $a=\{\lambda_1,\lambda_2,\rho_1,\rho_2\}$. Since the deuteron is a $J=1$ state, the angular dependence can explicitly be separated out,

$$\phi^{(M)}(p,a)=\left[\frac{2J+1}{2}\right]^{1/2}D^{J*}_{M\lambda}(\Omega_{\mathbf{p}})\phi(|\mathbf{p}|,p_0,a)\ , \tag{A13}$$

where

$$D^J_{\lambda'\lambda}(\Omega)=e^{-i\lambda'\varphi}d^J_{\lambda'\lambda}(\theta)e^{i\lambda\varphi} \tag{A14}$$

are the Wigner rotation matrices.[14] Using standard recoupling the states in Eq. (A12) labeled by J, M, λ_1, λ_2, ρ_1, and ρ_2 can be related to states labeled by $n=\{J,M,L,S\}$ and the total energy spin ρ, given by the combinations

$$+=(+,+),\quad -=(-,-)\ ,$$
$$e=[(+,-)+(-,+)]/\sqrt{2}\ , \tag{A15}$$
$$o=[(+,-)-(-,+)]/\sqrt{2}\ .$$

Denoting the recouplings to the above ρ-spin states as $C(\rho;\rho_1,\rho_2)$ and using the transformation matrix[35]

$$\langle J\lambda_1\lambda_2|JLS\rangle=\left[\frac{2L+1}{2J+1}\right]^{1/2}C^{LSJ}_{0\lambda\lambda}C^{1/2\,1/2S}_{\lambda_1-\lambda_2\lambda} \tag{A16}$$

we have the desired result

$$\phi_{n,a}(\mathbf{p},p_0)=\left[\frac{2L+1}{2}\right]^{1/2}C^{LSJ}_{0\lambda\lambda}C^{1/2\,1/2S}_{\lambda_1-\lambda_2\lambda}D^{J*}_{M\lambda}(\Omega_{\mathbf{p}})$$
$$\times C(\rho;\rho_1,\rho_2)\phi(|\mathbf{p}|,p_0,n,\rho)\ . \tag{A17}$$

The states $\phi_{n,m}(\mathbf{p},p_0)$ with $m=\{\lambda_1,\lambda_2,\rho\}$ are defined by Eq. (A17) without the coupling $C(\rho;\rho_1,\rho_2)$.

In the notation $^{2S+1}L^\rho_J$ of Gammel, Menzel, and Wortman,[36] the following eight states $\phi(|\mathbf{p}|,p_0,n,\rho)$ for the deuteron exist,

$$1{:}^3S^+_1,\ \ 2{:}^3D^+_1,\ \ 3{:}^3S^-_1,\ \ 4{:}^3D^-_1,$$
$$5{:}^1P^e_1,\ \ 6{:}^3P^o_1,\ \ 7{:}^1P^o_1,\ \ 8{:}^3P^e_1. \tag{A18}$$

The last two states are odd in p_0 and disappear in the case of the BSLT quasipotential.

An expansion of the two nucleon propagator $S_2(p,P)=S^{(1)}(\frac{1}{2}P+p)S^{(2)}(\frac{1}{2}P-p)$ can be made on the ρ-spin basis given in Eq. (A15). If the total ρ-spin states are given by $|\mathbf{p}\lambda_1\lambda_2\rho\rangle$ we may write

$$S_2(p,P)=\sum_{\rho\rho'}\Lambda_{\rho\rho'}(\mathbf{p})S_{\rho\rho'}(p,P)\ , \tag{A19}$$

where $\Lambda_{\rho\rho'}(\mathbf{p})=\sum_{\lambda_1\lambda_2}|\mathbf{p}\lambda_1\lambda_2\rho\rangle\langle\mathbf{p}\lambda_1\lambda_2\rho'|$. The scalar part of the two nucleon propagator $S_{\rho\rho'}(p,P)$ has the

form as given in Ref. 36 and is no longer dependent on the helicity.

A useful result is the property of

$$|\mathbf{p}\lambda_1\lambda_2\rho\rangle\phi_{n,m}(\mathbf{p},p_0) \tag{A20}$$

under a parity transformation. The free two particle states $|\mathbf{p}\lambda_1\lambda_2\rho_1\rho_2\rangle$ transform to

$$e^{2i\lambda\varphi}(-1)^{2s+\lambda}|\mathbf{p}\lambda_2\lambda_1\rho_2\rho_1\rangle \tag{A21}$$

if we reverse the sign of p, i.e., $\theta\rightarrow\pi-\theta$, $\varphi\rightarrow\varphi+\pi$, and $p_0\rightarrow -p_0$. Together with symmetry relations of the Clebsch-Gordan coefficients and Wigner rotations appearing in Eq. (A17) we get

$$|\mathbf{p}\lambda_1\lambda_2\rho\rangle\phi_{n,m}(\mathbf{p},p_0) \rightarrow(-1)^{L+S+2s}|\mathbf{p}\lambda_2\lambda_1\hat{\rho}\rangle\phi_{n,\hat{m}}(\mathbf{p},-p_0)\ , \tag{A22}$$

where $\hat{\rho}$ and $\hat{m}$ means that ρ_1 and ρ_2 and λ_1 and λ_2 are interchanged.

APPENDIX B

The scattering amplitude for elastic electron-deuteron scattering is given in the one-photon exchange approximation by

$$M=ie\bar{u}_{\lambda'}(\mathbf{k}')\gamma_\mu u_\lambda(\mathbf{k})\frac{1}{q^2}\langle P',M'|J_D^\mu|P,M\rangle\ , \tag{B1}$$

where the initial and final electrons are described by dirac spinors u_λ and $u_{\lambda'}$ with momenta $\mathbf{k}$ and $\mathbf{k}'$. P and P' are the four-momenta of the initial and final deuteron with polarizations M and M'. The deuteron current can be decomposed[37] into three scalar functions as follows form Lorentz covariance and time-reversal invariance and can be written in the following form:

$$\langle P',M'|J_D^\mu|P,M\rangle = -\frac{e}{2M^D}\left[(P'+P)^\mu\left[\varepsilon'^*\cdot\varepsilon F_1-\varepsilon'^*\cdot q\varepsilon\cdot q\frac{F_2}{2M_D^2}\right] -(\varepsilon'^{*\mu}\varepsilon\cdot q-\varepsilon'^*\cdot q\varepsilon^\mu)G_1\right]\ , \tag{B2}$$

where we suppressed the dependence on the momenta and polarization of the polarization four vectors $\varepsilon(P,M)$ and $\varepsilon(P',M')$ of the initial and final deuteron which are defined by

$$\begin{aligned}&\varepsilon^*(P,M)\cdot\varepsilon(P,M')=-\delta_{M,M'}\ ,\\ &\sum_M\varepsilon_\mu^*(P,M)\varepsilon_\nu(P,M)=-g_{\mu\nu}+\frac{P_\mu P_\nu}{M_D^2}\ ,\\ &P\cdot\varepsilon(P,M)=0\ .\end{aligned} \tag{B3}$$

The scalar functions are connected to the charge, quadrupole and magnetic form factors, by the relations

$$\begin{aligned}&F_C=F_1+\tfrac{2}{3}\eta[F_1+(1+\eta)F_2-G_1]\ ,\\ &F_Q=F_1+(1+\eta)F_2-G_1,\quad F_M=G_1\ ,\end{aligned} \tag{B4}$$

where $\eta=-q^2/4M_D^2$ and $F_C(0)=1$, $F_Q(0)=M_D^2Q_d$ and $F_M(0)=(M_D/M_N)\mu_d$. Q_d and μ_d are the quadrupole and magnetic moment of the deuteron. These form factors can be related to the current matrix elements $\langle P',M'|J_D^\mu|P,M\rangle$. In the Breit frame Eq. (B2) gives the relations

$$\begin{aligned}F_C&=\frac{1}{3e\sqrt{1+\eta}}(\langle P',M'|J_0^D|P,M\rangle\delta_{M,0}\delta_{M',0} +\langle P',M'|J_0^D|P,M\rangle\delta_{M\pm1,0}\delta_{M'\pm1,0})\ ,\\ F_Q&=\frac{1}{2\eta e\sqrt{1+\eta}}(\langle P',M'|J_0^D|P,M\rangle\delta_{M,0}\delta_{M',0} -\langle P',M'|J_0^D|P,M\rangle\delta_{M\pm1,0}\delta_{M'\pm1,0})\ ,\\ F_M&=\frac{-1}{e\sqrt{2\eta(1+\eta)}}\langle P',M'|J_+^D|P,M\rangle\delta_{M',M+1}\ .\end{aligned} \tag{B5}$$

The cross section for scattering of unpolarized electrons on unpolarized deuteron only depend on two form factors,

$$\frac{d\sigma}{d\Omega_e}=\sigma_{\text{Mott}}[A(q^2)+B(q^2)\tan^2\tfrac{1}{2}\theta_e]\ , \tag{B6}$$

where σ_{Mott} is the Mott cross section and θ_e the electron scattering angle. The electric and the magnetic form factors are defined by

$$\begin{aligned}&A(q^2)=F_C^2+\tfrac{8}{9}\eta^2F_Q^2+\tfrac{2}{3}\eta F_M^2\ ,\\ &B(q^2)=\tfrac{4}{3}\eta(1+\eta)F_M^2\ .\end{aligned} \tag{B7}$$

Electron scattering on polarized deuteron gives the tensor polarization[38] t_{20} which is defined by

$$t_{20}=-\sqrt{2}\frac{x(x+2)+y/2}{1+2(x^2+y)}\ , \tag{B8}$$

where

$$\begin{aligned}&x=\frac{2}{3}\eta\frac{F_Q}{F_C}\ ,\\ &y=\frac{2}{3}\eta\left[\frac{1}{2}+(1+\eta)\tan^2\left[\frac{\theta_e}{2}\right]\right]\frac{F_M^2}{F_C^2}\ .\end{aligned} \tag{B9}$$

[1]R. G. Arnold, B. T. Chertok, E. B. Dally, A. Grigorian, C. L. Jordan, W. P. Schütz, R. Zdarko, F. Martin, and B. A. Mecking, Phys. Rev. Lett. **35**, 776 (1975).
[2]S. Auffret *et al.*, Phys. Rev. Lett. **54**, 649 (1985).
[3]R. G. Arnold *et al.*, Phys. Rev. Lett. **58**, 1723 (1987).
[4]M. J. Zuilhof and J. A. Tjon, Phys. Rev. C **22**, 2369 (1980).
[5]J. A. Tjon and M. J. Zuilhof, Phys. Lett. **84B**, 31 (1979); M. J. Zuilhof and J. A. Tjon, Phys. Rev. C **24**, 736 (1981).

[6]R. G. Arnold, C. E. Carlson, and F. Gross, Phys. Rev. C **21**, 1426 (1980).
[7]C. J. Horowitz, *Proceedings of the Workshop on Relativistic Nuclear Many Body Physics,* Columbus, Ohio, 1988, edited by B. C. Clark, R. J. Perry, and J. P. Vary (World Scientific, Singapore, 1989).
[8]E. Hummel and J. A. Tjon, Phys. Rev. Lett. **63**, 1788 (1989).
[9]M. Gari and H. Hyuga, Nucl. Phys. **A264**, 409 (1976).
[10]W. P. Sitarski, P. G. Blunden, and E. L. Lomon, Phys. Rev. C **36**, 2479 (1987).
[11]M. Chemtob, E. Moniz, and M. Rho, Phys. Rev. C **10**, 344 (1974).
[12]R. Blankenbecler and R. Sugar, Phys. Rev. **142**, 1051 (1966); A. A. Logunov and A. N. Tavkhelidze, Nuovo Cimento **29**, 380 (1963).
[13]A. C. Hearn, REDUCE user's manual, Rand Corporation, Santa Monica (1984).
[14]M. E. Rose, *Elementary Theory of Angular Momentum* (Wiley, New York, 1957).
[15]J. Fleischer and J. A. Tjon, Nucl. Phys. **B84**, 375 (1975); Phys. Rev. D **15**, 2537 (1977); **21**, 87 (1980).
[16]B. Gobbi, J. L. Rosen, H. A. Scott, S. L. Shapiro, L. Strawczynski, and C. M. Meltzer, Phys. Rev. Lett. **33**, 1450 (1974).
[17]D. Berg *et al.*, Phys. Rev. Lett. **44**, 706 (1980).
[18]M. J. Zuilhof and J. A. Tjon, Phys. Rev. C **26**, 1277 (1982).
[19]J. Keyne, D. M. Binnie, J. Carr, N. C. Debenham, A. Duane, D. A. Garbutt, W. G. Jones, I. Siotis, and J. G. McEwen, Phys. Rev. D **14**, 28 (1976).
[20]D. E. Andrews, Y. Fukushima, J. Harvey, F. Lobkowicz, E. N. May, C. A. Nelson, Jr., and E. H. Thorndike, Phys. Rev. Lett. **38**, 198 (1977).
[21]M. Gari and W. Krümpelmann, Z. Phys. **322**, 689 (1985); M. Gari, Proceedings of the Workshop on Electro-nuclear Physics with Internal Targets, 1987 (unpublished).
[22]G. Höhler, E. Pietarinen, I. Sabba-Stefanescu, F. Barkowski, G. G. Simon, V. H. Walther, and R. D. Wendling, Nucl. Phys. **B114**, 505 (1976).
[23]F. Iachello, A. D. Jackson, and A. Landé, Phys. Lett. **43B**, 191 (1973).
[24]M. J. Zuilhof, thesis, Utrecht, 1981.
[25]P. L. Chung, F. Coester, B. D. Keister, and W. N. Polyzou, Phys. Rev. **37**, 2000 (1988).
[26]S. Platchkov *et al.*, Nucl. Phys. **A510**, 740 (1990).
[27]P. L. Chung, B. D. Keister, and F. Coester, Phys. Rev. C **39**, 1544 (1989).
[28]M. E. Schulze *et al.*, Phys. Rev. Lett. **52**, 597 (1984).
[29]J. A. Tjon, Nucl. Phys. **A463**, 157c (1987).
[30]L. L. Frankfurt, I. L. Grach, L. A. Kondratyuk, and M. I. Strikman, Phys. Rev. Lett. **62**, 387 (1989).
[31]R. Dymarz and F. C. Khanna, Phys. Rev. Lett. **56**, 1448 (1986).
[32]J. J. Kubis, Phys. Rev. D **6**, 547 (1972).
[33]J. Fleischer, J. Comput. Phys. **12**, 112 (1973).
[34]J. D. Bjorken and S. D. Drell, *Relativistic Quantum Fields* (McGraw-Hill, New York, 1965).
[35]M. Jacob and G. C. Wick, Ann. Phys. (N.Y.) **7**, 404 (1959).
[36]J. L. Gammel, M. T. Menzel, and W. R. Wortman, Phys. Rev. D **3**, 2175 (1971).
[37]M. Gourdin, Nuovo Cimento **28**, 533 (1963).
[38]M. I. Haftel, L. Mathelitsch, and H. F. K. Zingl, Phys. Rev. C **22**, 1285 (1980).